

Tailor Made Mie Scattering Color Filters Made by Size-Tunable Titanium Dioxide Particles

Min Chiao Tsai,[†] Tsung Lin Tsai,[‡] Cheng Te Lin,[†] Rei Jei Chung,[†] Hwo Shuenn Sheu,[§] Hsin Tien Chiu,^{||} and Chi Young Lee^{*,†}

Department of Materials Science and Engineering, National Tsing Hua University, Hsinchu, Taiwan, Institute of Basic Medical Sciences, National Cheng Kung University, Tainan, Taiwan, Synchrotron Radiation Research Center, Hsinchu, Taiwan, and Department of Applied Chemistry, National Chiao Tung University, Hsinchu, Taiwan

Received: August 20, 2007; In Final Form: November 18, 2007

Particles with sizes ranging from nanoscale to microscale were synthesized by the reaction of titanium isopropoxide (TTIP) with acetic, butyric, valeric, or octanoic acids. When acetic acid was used, anatase nanoparticles with diameters of approximately 15 nm were obtained while the other carboxylic acids yielded amorphous submicron-sized spheres. Moreover it is possible to adjust the particle size of the powders since it is proportional to the length of the alkyl group on the carboxylic acids used. When submicron-sized particles were coated on a transparent substrate (quartz or glass), different wavelengths of light were scattered. Thus color filters with specific wavelengths could easily be made by coating powders synthesized from specific carboxylic acids on the transparent substrate.

1. Introduction

In the past few decades, titanium-containing materials such as H_2TiO_3 ,¹ titanium carboxylate,² and especially TiO_2 have attracted a lot of interest due to numerous applications in photocatalysts,³ Li ion batteries,⁴ solar cells,⁵ and biomaterials.⁶ Furthermore, researchers also paid much attention to optical applications due to unique properties of TiO_2 , which include high refractive indices (2.57, 2.95, and 2.0 ~ 2.4 for anatase, rutile, and amorphous phases respectively)^{7–8} and wide band gaps (3.2 and 3.0 for anatase and rutile respectively).⁷ This makes TiO_2 film suitable for many applications, such as planar waveguides,⁹ antireflection coatings,¹⁰ and electrochromic displays.¹¹ Unlike usual thin film devices, 1-D multilayer stacks of porous films, known as Bragg stacks, have also been reported to provide a novel color-adjustable device.¹² The porous films stack together and change color by immersing into different solvents or changing their thickness.

Among recent researches, most periodic structures were prepared by using template methods. The synthesis of micron spheres polystyrene (PS) is very well-established, which makes it the most popular material for the template. However the usage of PS spheres still has some issues regarding the cost and stringent process conditions. In order to avoid defects, such as vacancies and boundaries in the layers, a highly uniform-sized mono-dispersed PS solution is required, which is very expensive. PS monolayer or multilayer coatings need to be applied meticulously by dip coating or spin coating;¹³ hence, it is time-consuming.

Here, we report a novel and straightforward method to synthesize uniform particles ranging from nanoscale to microscale with carboxylic acids as additives. Particle size can be

crudely controlled using different types of acid, while fine-tuning can be done by changing the volume of acid used. Moreover, the particles can easily be coated onto a transparent substrate to act as a simple color filter. Unlike structure color filters, which take advantage of the Bragg diffraction of periodic structures, these easily made filters work by light scattering off particles in the coating. Since scattering can occur on randomly spread particles, precise periodic structures are not required, making the coating process very easy. In addition, the precursor used in this study, titanium isopropoxide (TTIP), is also widely used in the sol–gel process and is therefore much cheaper than PS solutions.

2. Experimental Section

In our work, particles of various sizes were synthesized using titanium isopropoxide (TTIP, 97%, Aldrich) and various carboxylic acids in anhydride alcohol. Four carboxylic acids—glacial acetic, butyric (99%), valeric (99%), and octanoic (99.5%) acids, were all purchased from the Aldrich Company and used directly without any pretreatment.

A typical synthesis procedure of smallest TiO_2 particles (~15 nm) is as follows. Acetic acid (3.75 mL, 65 mmol) was injected into the 25 mL anhydride ethanol, followed by the addition of 0.3 mL (1 mmol) TTIP. The solution was then heated at 85 °C for 6 h under reflux in air. After that, hydrolysis and condensation were initiated by adding a 7 mL solution consisting of 2 mL DI water and 5 mL ethanol causing the particles to gradually precipitate over 4 h, turning the solution turbid. The precipitate was recovered by centrifuging and decanting of the liquid. It was then washed several times with ethanol and DI water, with the centrifuging and decanting process repeated after every wash. The residual ethanol and DI water were then pumped out in a vacuum system.

The remaining preparation of the submicron (<1 μm) and micron spheres (>1 μm) is almost the same procedure as described above except the kind of acid and the volume of water used. Different volumes of butyric (0.3~1.25 mL), valeric

* To whom correspondence should be addressed. E-mail: cylee@mx.nthu.edu.tw. Tel: +886 3 5715131-42570.

[†] National Tsing Hua University.

[‡] National Cheng Kung University.

[§] Synchrotron Radiation Research Center.

^{||} National Chiao Tung University.

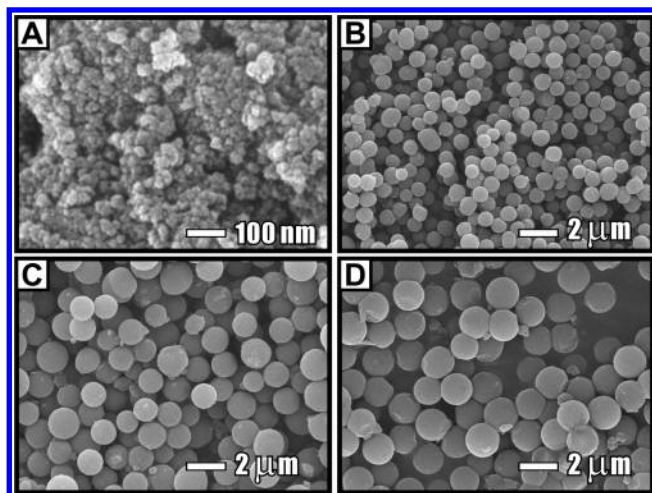


Figure 1. SEM images of the particles obtained from different conditions. (A) 15 nm nanoparticles obtained with acetic acid. (B) Submicron spheres smaller than $1 \mu\text{m}$ obtained with butyric acid. (C) Micron spheres larger than $1 \mu\text{m}$ synthesized with valeric acid. (D) Micron spheres larger than $2 \mu\text{m}$ synthesized with octanoic acid.

(0.5~2 mL) and octanoic (0.5~2 mL) acids were injected into the solvent and 1 mL water was added instead of 2 mL. Large amount of powders precipitated in 10 min to 2 h and the total reaction time was 2.5 h.

For UV-vis measurements and the color tests, a small amount TiO_2 powders were put into a quartz cuvette or a glass bottle then rolled mildly to coat TiO_2 powder on the interior wall of the bottle. Furthermore, the TiO_2 powders can also be coated on a flexible plastic sheet by spreading and shaking the powder on the sheet. The easy-made flexible color filter was shown in Figure S 1. Besides, in coverage test, we adopted the method reported in the literature¹⁴ to obtain monolayer TiO_2 film on the substrates by dipping substrate into the solution with floating spheres on the surface. The solution was prepared by dispersing 0.011 g spheres with 623 nm in diameter in 2 mL ethanol. Then, 250, 175, and 150 μL of the solution were dropped in DI water carefully, and the different degree of floating spheres solution were obtained. A plastic or glass sheet was dipped into the solution with floating spheres on the surface to obtain a monolayer TiO_2 coated substrate.

For characterizations, SEM images were taken with a JEOL-6500 scanning electron microscope. TEM images were obtained with a JEOL-2010 transition electron microscope with an accelerating voltage was of 200 keV. The particle size was examined by the Zetasizer Nano ZS, Malvern company. The spectra and photographs of scattered light were acquired using a Hitachi U-3010 spectrophotometer and a common digital camera respectively.

3. Results and Discussion

In this work, we synthesized uniform particles with sizes range from nanoscale to microscale by hydrolysis of titanium isopropoxide (TTIP) and carboxylic acids as additives.

Figure 1 shows the SEM images of the particles with different sizes, synthesized by utilizing different acids as additives. With the case of acetic acid (Figure 1A) was used, only the aggregates of very small particles can be seen. Moreover, the high-resolution transition electron microscopy (HRTEM; Figure 2A) shows a lumpy particle that is about 15 nm in diameter with small pores in. The particles were crystalline in anatase phase according to the distance of the lattice plane (101). If we replace acetic acid with butyric acid, submicron sized particles that range

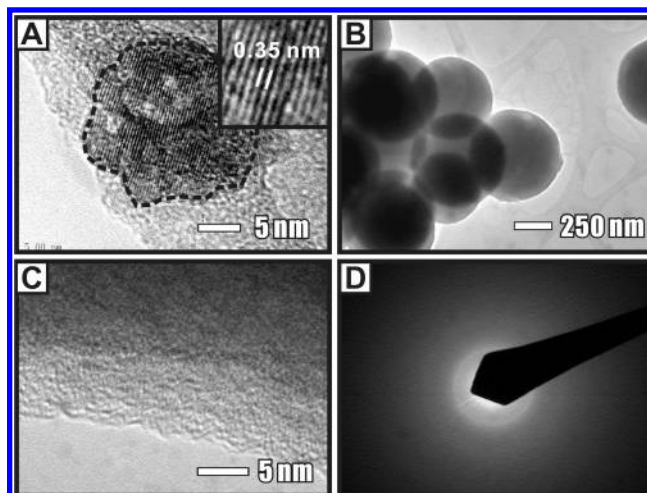
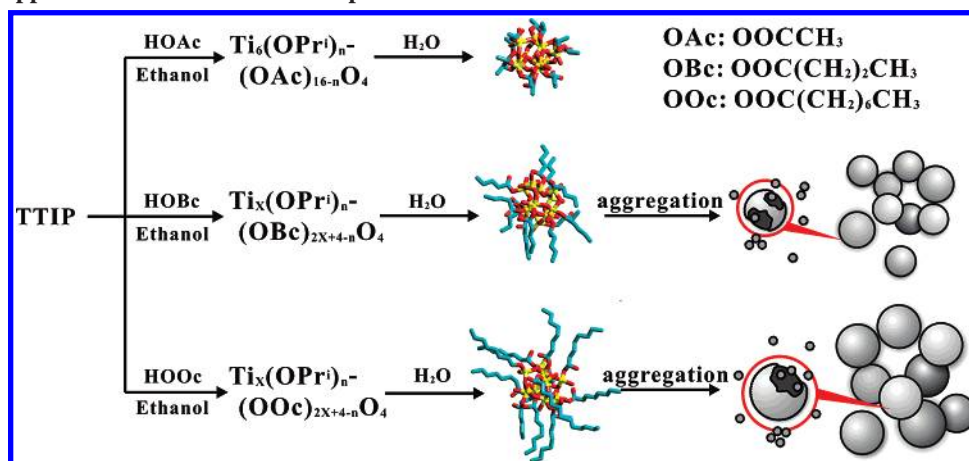


Figure 2. (A) TEM image of a nanoparticles synthesized using acetic acid. The lattices distance, 0.35 nm, indicates that the structure of the nanoparticle is anatase phase. (B) The TEM image of solid submicron spheres synthesized using butyric acid. (C and D) The HRTEM and ED images of the spheres in Figure 2B.

from 400 nm to $1 \mu\text{m}$ can be synthesized, as shown in Figure 1B. Figure 1, panels c and d, shows very large round smooth surface particles with usually over $1 \mu\text{m}$ in diameter that were synthesized with valeric acid or octanoic acid. In the sample with valeric acid, the sizes of the micron particles often range from 1 to $2 \mu\text{m}$, whereas those of octanoic acid usually exceed $2 \mu\text{m}$. Furthermore, the solid conglomeration different from the hollow spheres and mesoporous materials obtained from template and surfactant methods was characterized by TEM (Figure 2, panels B and C).¹⁵

According to above observations, we found a positive relationship between the length of the carboxylic acid's carbon chain and the size of the particles obtained. Here, we proposed a possible mechanism in Scheme 1. When we added carboxylic acid into the solution containing the TTIP, titanium carboxylate complex would be produced which was confirmed by the observation of a well-documented color change.¹⁶ As acetic acid reacted with TTIP, $\text{Ti}_6\text{O}_4(\text{OAc})_{16-4n}(\text{O}^i\text{Pr})_n$ was obtained and characterized in detail.¹⁷ Moreover, oligomers of TTIP and butyric or valeric acids are proposed, although the exact oligomeric structures were not outright elucidated.^{16,18,19} Thus, we also propose some small oligomers produced by the partial condensation with the water formed during esterification. Then, further hydrolysis and condensation took place after addition of water. The clusters bonded by carboxylate groups with carbon tails toward outside aggregate to form large particles, owing to the hydrophobicity of carbon tails. The evidence of carboxylate group bonded onto the surface of the micron spheres with carbon tails toward outside can be demonstrated by the IR spectrum of the micron spheres (Figure 3). The peaks at 1530 and 1444 cm^{-1} cohere with main characteristic of a carboxylate group bonded to titanium metal, whereas the C=O and C—O stretch of free carboxylic acid appear near 1730 and 1230 cm^{-1} . The three peaks at 2962, 2874, and 2931 cm^{-1} can be assigned to alkyl group stretching from the carbon tails.

Qin and co-workers also observed the aggregation and examined the solvophobic effect by thermodynamics simulation.^{20,21} In a colloidal solution, three kinds of interactions exist between nanoparticles: van der Waals forces, solvation, and electrostatic forces.²¹ In our system, the solvation force between nanoclusters is attraction due to the solvophobic effect between the hydrophobic carbon tails and ethanol. Since the nanoclusters

SCHEME 1: Supposed Mechanism in This Report^a

^a Alkoxycarboxylate of titanium was first formed by adding the acids into the TTIP solution and the n value in the alkoxycarboxylate formula depended on the mol ratio of the acids and the TTIP. At the next stage, small clusters were produced by hydrolysis and condensation of the alkoxycarboxylate after water was added. Finally, the small clusters merge to submicron and micron spheres by interparticle condensation due to hydrophobicity of carbon tails to reduce total energy.

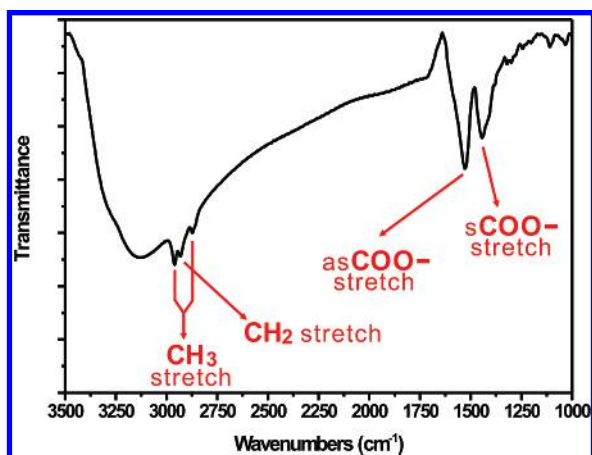


Figure 3. IR spectrum of the micron spheres. The absorbents appear at 1530 and 1444 cm^{-1} were assigned to the carboxylate groups bonded to titanium metal. This is the strong evidence that the spheres were surrounded by the carboxylate group.

TABLE 1: Diameter and Zeta Potential of Spheres Synthesized by Using Different Acids^a

butyric acid			valeric acid			octanoic acid		
V	D	ZP	V	D	ZP	V	D	ZP
0.5	462	-7.36	0.5	831	-3.06	0.5	1227	-4.07
0.75	623	-6.05	1.0	1270	-1.68	1.0	1700	-10.7
1.1	674	-9.18	1.5	1290	2.39	1.5	2213	-1.97
1.25	772	-7.87	2.0	1580	-3.07	2.0	3010	-3.98

^a V: volume (mL) D: diameter (nm); ZP: zeta potential (mV).

are practically uncharged (zeta potential of micron spheres is nearly zero as shown in Table 1), the electrostatic force is insignificant. Thus, the overall interaction between the nanoclusters is attractive, making the nanoclusters self-assemble to the submicron and micron-sized spheres. Increasing the length of the carbon tail would lead to an increase in hydrophobicity, which is less favorable in the ethanol solution. Hence, the clusters tended to agglomerate together to reduce free energy resulting in larger particles.

The carboxylic acids in our experiments not only dominate particle size but also crystalline phase. In Figure 4, the X-ray diffraction pattern (XRD) shows the nanoparticles synthesized with acetic acid in anatase phase. Although, the submicron spheres and micron spheres (not shown here) synthesized with

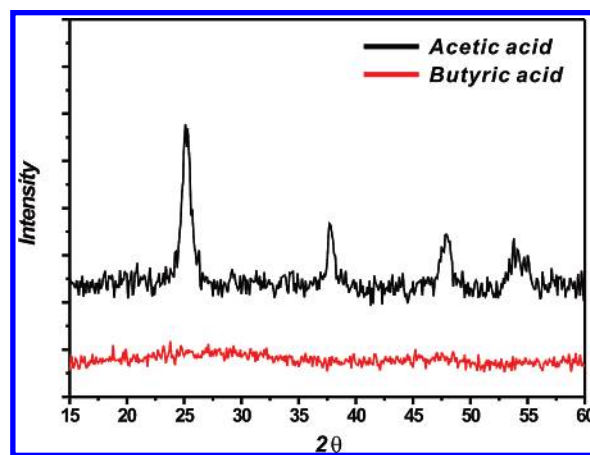


Figure 4. XRD patterns of the particles. Top line presents the nanoparticles obtained from acetic acid have anatase phase according to the peaks at 25, 37.5, and 47.5 degrees, which can be assigned to the (101), (004), and (200) of anatase phase, respectively. Bottom line shows the submicron spheres are amorphous phase and the micron spheres obtained from valeric and octanoic acids also show the same results.

long chain carboxylic acid were all in amorphous phase. The amorphous structures are also conformed by the blur ring pattern of electron diffraction (Figure 2D). Zhang and co-workers²² reported that crystalline anatase can be synthesized by the hydrolysis of titanium ethoxide using acetic acid as an additive at 400 °C. In our experiments, purely anatase phase products were observed at 85 °C.

It is generally known, acidity (or pH values) of the acids and affinity to titanium atom are two important factors that affect the microstructure of the titanium oxide formed. It has been extensively reported that rutile formation can be facilitated in strong acids with large K_a , like HCl and HNO₃.²³ However, it is stable for anatase to form in strong field ligands, e.g., SO₄²⁻ and CH₃COO⁻.^{24,25} The acids we used in our experiments all have similar K_a values,²⁶ but the microstructures of the powders obtained are quite different. Thus, we proposed that the affinity of acid to titanium atom has a critical effect on crystallinity instead of acidity in our experiments. It is well-known that acetic acid can retard the hydrolysis rate because of its strong affinity to a titanium atom.²⁴ According to the estimation of partial charges,²⁷ a butyrate group has positive partial charge ($\delta(\text{CH}_3-$

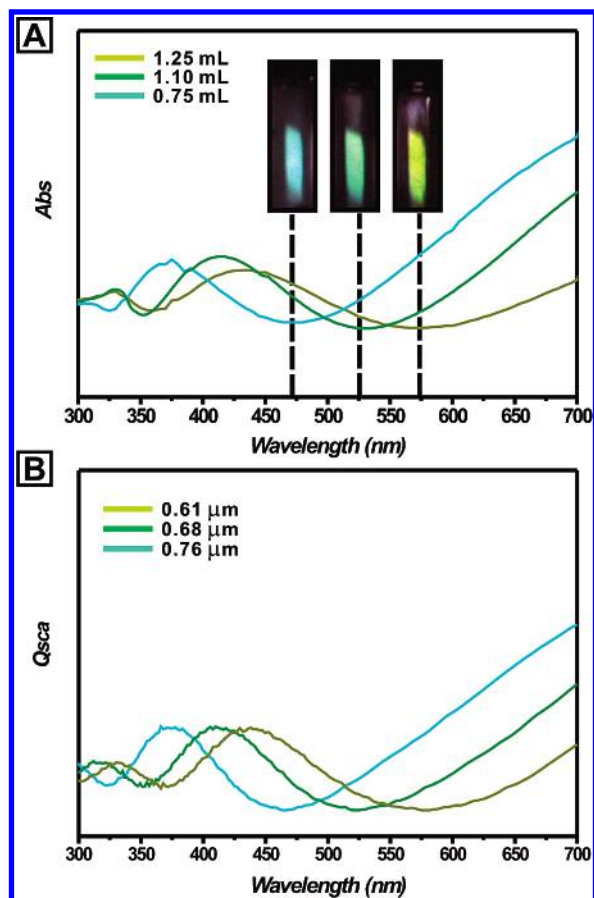


Figure 5. (A) UV-vis spectra of the submicron spheres acquired from the different volume of butyric acid. Cyan, green and yellow-green lines denote the scattering property of the powders obtained by using 0.75, 1.10, and 1.25 mL butyric acid, respectively. Colorful photographs show that the light transited through the cuvettes which are coated with the powders presented different colors. (B) the theoretical Mie scattering spectra. Simulated UV-vis spectra for powders of diameters 0.61, 0.68, and 0.76 μm were created using MiePlot and the values corresponded to the spectra of powders obtained from the reactions with 0.75, 1.10, and 1.25 mL butyric acid respectively.

$\text{CH}_2\text{CH}_2\text{COO}) = 0.10$) and an acetate group has negative partial charge ($\delta(\text{CH}_3\text{COO}) = -0.18$). Species with negative partial charges have stronger affinity to a titanium atom (partial charge is about 0.7) than those with positive partial charges in the partial charge model (PCM). Thus the acetate group strongly bonded to titanium metal retarding the hydrolysis rate, resulting in a crystalline anatase TiO_2 powder. On the other hand, butyrate groups with positive partial charge weakly bonded to titanium metal, so TiO_2 precipitated much faster than that with acetic acid to form amorphous powders (see experimental).

According to the IR analysis, the micron spheres were surrounded by a layer of organic fragments. This organic layer makes the micron spheres adhere easily to many kinds of substrates such as glass, quartz, plastics and even papers, resulting in the formation of a monolayer coating on the substrate. The coverage of the monolayer TiO_2 films were prepared by the method reported by Rybczynski.¹⁴ Figure S2 shows the SEM images of the substrate with different TiO_2 coverage. We found that the spheres were arranged randomly on plastic sheets along with some aggregates. The coverage estimated from the SEM images by an analytical software, Image-Pro Plus 6.0, were 30.3%, 57.4%, and 67.5% for the sample obtained from 150, 175, and 250 μL , respectively.

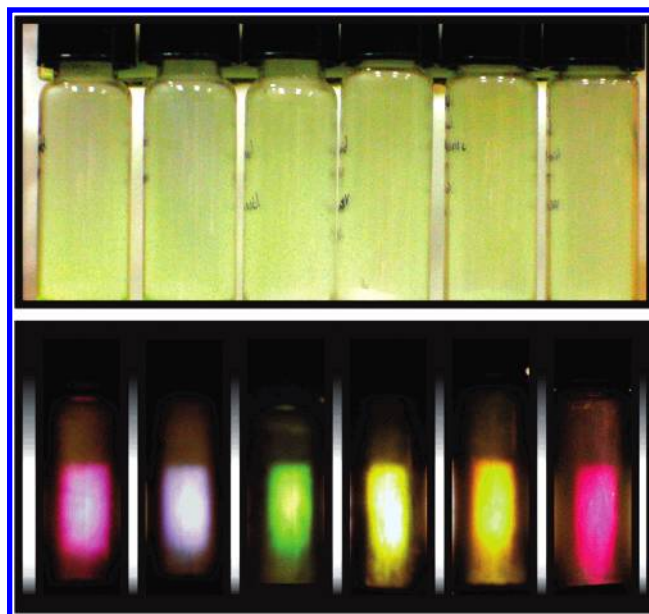


Figure 6. Top: The original spheres coated on glass bottles synthesized with valeric acid. All spheres synthesized with different conditions (0.36~0.47 mL) have white color like usual TiO_2 powders. Bottom: When turn on a back light, multicolored light could be observed through the bottles by Mie scattering (from left to right, purple, blue, green, yellow-green, yellow, and red, respectively).

Furthermore, we found those powders have a very interesting optical property. When white light passes through cuvettes with their interior walls coated with the spheres synthesized with valeric acid or different volume of butyric acid different colors were observed, as shown in Figure 5A. Coating cuvettes with powders obtained from 0.75, 1.10, and 1.25 mL butyric acid yielded cyan, green and yellow-green respectively. The whole spectra could be also obtained by using different amount of valeric acid (as shown in Figure 6).

The UV-vis spectra of those powders are shown in Figure 5A. The local minimum in the spectra marked by the dashed lines represents the wavelength of light transmitted through the powders. The phenomena can be well interpreted by the Mie scattering theory originated from destructive and constructive interference of transmission and refraction of light through the particle and diffraction and reflection of light from the particle surface.²⁷ Interestingly, we did not clearly observe an important feature of Mie scattering, which should result in sharp jagged peaks in scattering intensity in our spectra, often called Mie resonances or morphology dependent resonances (MDR).²⁸ MDR are usually used to monitor the growth or evaporation of the size of particles.²⁹ All UV-vis spectra obtained were smooth in our cases and it is the result of the wide particle size distribution of our samples.

Figure 5B shows theoretical Mie scattering spectra calculated by MiePlot 3.5.10.³⁰ The simulated curves match our experimental spectra well, although there is a small inconsistency at short wavelengths area due to deviations in analysis preparation. Simulated UV-vis spectra for powders of diameters 0.61, 0.68, and 0.76 μm were created using MiePlot and the values corresponded to the spectra of powders obtained from the reactions with 0.75, 1.10, and 1.25 mL butyric acid respectively. The sizes of the powders obtained from 0.75, 1.10, and 1.25 mL butyric acid were shown in Table 1. The average diameters of the particles agreed with the estimated particle diameters.

The UV-vis spectra of TiO_2 films with different coverage are shown in Figure 7A. It can be seen that the increase in coverage does not lead to a linear increase in absorbance over

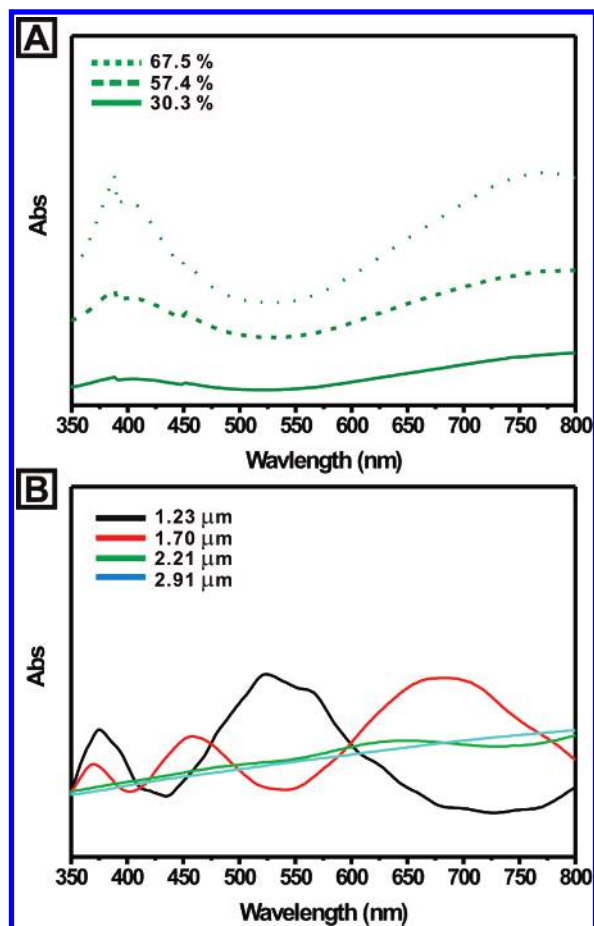


Figure 7. (A) UV-vis spectra of monolayers with different coverage. The dot, dash, and solid lines represent the spectra of 67.5%, 57.4%, and 30.3% coverage on plastic sheets, respectively. (B) the UV-vis spectra of different spheres ranged from 1 to 3 μm . The black, red, green and blue denote the spectra acquired from 1.23, 1.70, 2.21, and 2.91 μm , respectively.

the whole spectrum but an obvious peak at some specific wavelengths. This is because the absorbance is expressed by a log scale. If the log scale was converted to a percentage scale, the absorbance variation of the whole spectrum becomes constant in the range between 350 and 800 nm. Besides, the high-coverage sheet appears to be a deeper color than the low-coverage one when observed with the naked eye.

In Mie scattering, the amplitude of Q_e (extinction efficiency factor) decreases gradually as x (size parameter, $x = 2\pi r/\lambda$) increases and approaches a constant value. This means that the strongest scattering moves to long wavelengths with increasing size and the curves of spectrum in the visible light region will flatten gradually. Larger spheres with diameter in 1.2–3.0 μm synthesized from octanoic acid were also examined for their optical properties. The UV-vis spectra of the TiO_2 film with large particles are shown in Figure 7B. As we can see, UV-vis spectrum shows a red shift as particle size increases. Although, the minimum shifts away from the visible light region, the second minimum moves into the visible light region. The second minimum can also selectively scatter different wavelengths of light to display filter properties. On the other hand, the volume extinction coefficient (σ_e) in a polydispersed system is significantly affected by the size distribution of the spheres.³¹ The broader the distribution, the smaller the extinction coefficient in the visible light region and filter property disappears. In our experiments, the bigger the spheres obtained, the broader the distribution (Supporting Information, Table S1). As shown

in the Figure 7B, the absorbance curves of the large particle, green and blue, are flat and filter property cannot be seen by the naked eye.

4. Conclusions

In conclusion, a novel synthesis of particles with sizes ranging from nanoscale to micron-scale with carboxylic acids as additives was reported. The length of the alkyl group and the quantity of carboxylic acids affected the microstructures and particle size of the products. When acetic acid was used as an additive, stronger affinity between the acetate group and the central titanium atom retarded the reaction to form fine anatase powder. On the other hand, when carboxylic acids with long alkyl groups were used as additives, weak interactions between the carboxylate groups and central titanium atom increased the reaction rate to form large amounts of amorphous powders. Moreover, the particle size could be adjusted by choosing carboxylic acids with alkyl groups of different length. Due to their hydrophobicities, the longer the carbon tails on the acids used, the larger the particles that were obtained.

The differently sized particles perform different scattering effects to make them being a color filter. We successfully adjusted the colors passing through the filter by coating the powders obtained from the synthesis with various quantities of butyric acid on the glass. The relationship between observed color passing through the coating and the particle size could be well interpreted by the Mie scattering theory. The transmission spectra of variously sized particles simulated by MiePlot agree with the experimental spectra very well. Thus, color filters for specific wavelengths could easily be made by coating powders synthesized with different carboxylic acids on the transparent substrate.

Acknowledgment. The authors would like to thank the National Science Council, R.O.C. Taiwan and Synchrotron Radiation Research Center, Taiwan for financially supporting this research under Contract No. NSC 94-2113-M-007-028.

Supporting Information Available: Figure S1. The pictures show that we prepared a flexible scattering color filter with large area quickly by coating three different size spheres on a flexible plastic sheet with adhesive property of spheres. Figure S2. The SEM images show three monolayers having different coverage, 30.3%, 57.4%, and 67.5% from top to bottom, respectively. Table S1. The sizes and standard deviations of spheres calculated from SEM images. This material is available free of charge via the Internet at <http://pubs.acs.org>.

References and Notes

- (1) (a) Chen, Q.; Zhou, W.; Du, G. H.; Peng, L. M. *Adv. Mater.* **2002**, *14*, 1208. (b) Zhang, S.; Chen, Q.; Peng, L. M. *Phys. Rev. B* **2005**, *71*, 014104.
- (2) (a) Doeuff, S.; Dromzee, Y.; Taulelle, F.; Sanchez, C. *Inorg. Chem.* **1989**, *28*, 4439. (b) Lei, X.; Shang, M.; Fehlner, T. P. *Organometallics* **1997**, *16*, 5289. (c) Boyle, T. J.; Alam, T. M.; Tafoya, C. J.; Scott, B. L. *Inorg. Chem.* **1998**, *37*, 5588.
- (3) (a) Asahi, R.; Morikawa, T.; Ohwaki, T.; Aoki, K.; Taga, Y. *Science* **2001**, *293*, 269. (b) Shahed Mofareh Al-Shahry Khan, U. M.; Ingler, B. William, Jr. *Science* **2001**, *297*, 2243. (c) Sakthivel, S.; Kisch, H. *Angew. Chem., Int. Ed.* **2003**, *42*, 4908. (d) Yu, J. C.; Ho, W.; Yu, J.; Yip, H.; Wong, P. K.; Zhao, J. *Environ. Sci. Technol.* **2005**, *39*, 1175.
- (4) (a) Koudriachova, M. V.; Harrison, N. M. *J. Mater. Chem.* **2006**, *16*, 1973. (b) Koudriachova, M. V.; Harrison, N. M.; de Leeuw, S. W. *Phys. Rev. Lett.* **2001**, *86*, 1275.
- (5) (a) Ma, T.; Akiyama, M.; Abe, E.; Imai, I. *Nano. Lett.* **2005**, *5*, 2543. (b) Ghicov, A.; Macak, J. M.; Tsuchiya, H.; Kunze, J.; Haeublein, V.; Frey, L.; Schmuki, P. *Nano. Lett.* **2006**, *6*, 1080.

- (6) (a) Liu, X.; Zhao, X.; Ding, C.; Chu, P. K. *Appl. Phys. Lett.* **2006**, *88*, 013905. (b) Cho, M.; Chung, H.; Choi, W.; Yoon, J. *Appl. Environ. Microbiol.* **2005**, *71*, 270.
- (7) Diebold, U. *Surf. Sci. Rep.* **2003**, *48*, 53.
- (8) (a) Meng, L. J.; Teixeira, V.; Cui, H. N.; Placido, F.; Xu, Z., dos Santos, M. P. *Appl. Surf. Sci.* **2006**, *252*, 7970. (b) Abdel-Aziz, M. M.; Yahia, I. S.; Wahab, L. A.; Fadel, M.; Afifi, M. A. *Appl. Surf. Sci.* **2006**, *252*, 8163.
- (9) Qi, Z. M.; Itoh, K.; Murabayashi, M.; Lavers, C. R. *Opt. Lett.* **2000**, *25*, 1427.
- (10) Vicente, G. S.; Gutierrez, M. T. *Thin Solid Film* **2002**, *403–404*, 335.
- (11) Olesik, J. W.; Kinzer, J. A. *J. Appl. Phys. Part 1* **1997**, *36*, 4423.
- (12) Choi, S. Y.; Mamak, M. G.; von Freymann, G.; Chopra, N.; Ozin, G. A. *Nano. Lett.* **2006**, *6*, 2456.
- (13) (a) Graugnard, E.; Gailliot, D. P.; Dunham, S. N.; Neff, C. W.; Yamashita, T.; Summers, C. J. *Appl. Phys. Lett.* **2006**, *89*, 181108. (b) Choi, S. Y.; Lee, B.; Carew, D. B.; Mamak, M.; Peiris, F. C.; Speakman, S.; Chopra, N.; Ozin, G. A. *Adv. Funct. Mater.* **2006**, *16*, 1713.
- (14) Rybczynski, J.; Ebels, U.; Giersig, M. *Colloid Surf. A – Physico-chem. Eng. Asp.* **2003**, *219*, 1.
- (15) (a) Wang, J.; Xiao, Q.; Zhou, H.; Sun, P.; Yuan, Z.; Li, B.; Ding, D.; Shi, A. C.; Chen, T. *Adv. Mater.* **2006**, *18*, 3284. (b) Caruso, F. *Adv. Mater.* **2001**, *13*, 11.
- (16) Dunuwila, D. D.; Gagliardi, C. D.; Berglund, K. A. *Chem. Mater.* **1994**, *6*, 1556.
- (17) (a) Doerff, S.; Dromzee, Y.; Sanchez, C. C. *C. R. Acad. Paris* **1989**, *308*, 1409. (b) Laaziz, I.; Gagliardi, C. D.; Durand, J.; Cot, L.; Joffre, J. *Acta, Crystallogr., Sect. C* **1990**, *46*, 2332.
- (18) Severin, K. G.; Ledford, J. S.; Torgerson, B. A.; Berglund, K. A. *Chem. Mater.* **1994**, *6*, 890.
- (19) Boyle, T. J.; Tafuya, C. J.; Scott, B. L. *Abstr. Pap.- Am. Chem. Soc.* **1996**, *211* (part 1), 62-INOR.
- (20) (a) Xia, Y.; Gates, B.; Yin, Y.; Lu, Y. *Adv. Mater.* **2000**, *12*, 693. (b) Ocana, M.; Rodriguez-Clemente, R.; Serna, C. J. *Adv. Mater.* **1995**, *7*, 212.
- (21) (a) Rabani, E.; Egorov, S. A. *J. Chem. Phys.* **2001**, *115*, 3437. (b) Rabani, E.; Egorov, S. A. *Nano. Lett.* **2002**, *2*, 69. (c) Qin, Y.; Fichthorn, K. A. *J. Chem. Phys.* **2003**, *119*, 9745.
- (22) Zhang, H.; Finnegan, M.; Banfield, J. F. *Nano. Lett.* **2001**, *1*, 81.
- (23) (a) Yamabi, S.; Imai, H. *Chem. Mater.* **2002**, *14*, 609. (b) Hoffmann, M. R.; Martin, S. T.; Choi, W.; Bahnemann, D. W. *Chem. Rev.* **1995**, *95*, 69.
- (24) Wu, M.; Lin, G.; Chen, D.; Wang, G.; He, D.; Feng, S.; Xu, R. *Chem. Mater.* **2002**, *14*, 1974.
- (25) Colón, G.; Sánchez-España, J. M.; Hidalgo, M. C.; Navío, J. A. *J. Photochem. Photobiol. A-Chem.* **2006**, *179*, 20.
- (26) acetic acid: K_a 1.74–5, butyric acid: K_a 1.48–5, octanoic acid: K_a 1.29–5.
- (27) Venz, P. A.; Klopogge, J. T.; Frost, R. L. *Langmuir* **2000**, *16*, 4962.
- (28) Olesik, J. W.; Kinzer, J. A. *Spectrosc. Acta Part A* **2006**, *61*, 696.; Ashkin, A.; Dziedzic, J. M. *Appl. Opt.* **1981**, *20*, 1803.
- (29) Richardson, C. B.; Hightower, R. L.; Pigg, A. L. *Appl. Opt.* **1986**, *25*, 1226.
- (30) Laven, P. MiePlot 3.5.01 <http://www.philiplaven.com/mieplot.htm>.
- (31) Jennings, S. G.; Pinnick, R. G.; Auvermann, H. J. *Appl. Opt.* **1978**, *24*, 3922.